1871
ИнБЮМ – IBSS

Морской биологический журнал
Marine Biological Journal
2024, vol. 9, no. 1, pp. 51–69
https://marine-biology.ru

UDC 581.526.325(268.45.02)

LOCALIZATION OF PHYTOPLANKTON EARLY SPRING BLOOM SPOTS IN THE PELAGIC ZONE OF THE BARENTS SEA

© 2024 **P. Makarevich, V. Vodopyanova, A. Bulavina, P. Vashchenko, A. Namyatov, and I. Pastukhov**

Murmansk Marine Biological Institute of the Russian Academy of Sciences, Murmansk, Russian Federation
E-mail: *makarevich@mmbi.info*

Received by the Editor 01.04.2022; after reviewing 26.07.2022;
accepted for publication 09.10.2023; published online 22.03.2024.

Atlantification of the Barents Sea leads to a decrease in the area of ice cover and an increase in the ice-free period. This process affects the entire pelagic ecosystem of the Barents Sea, where the main part of the annual primary production of phytoplankton is formed during the spring bloom. Chlorophyll *a* concentration reflects changes in phytoplankton biomass and can serve as an indicator of its production characteristics. In the spring of 2021, hydrological characteristics of water masses, as well as the distribution of concentrations of chlorophyll *a* and nutrients, were studied in the ice-free water area of the Barents Sea. The year of 2021 was characterized by negative ice cover anomalies. The location and length of the areas of increased (or decreased) chlorophyll *a* concentrations were consistent with the alternation of water masses. Separate spots of early spring bloom were identified – in coastal waters in the southeastern and southwestern Barents Sea. In late March and early April 2021, maximum chlorophyll *a* concentrations in coastal waters reached values of about 1 mg·m^{-3}. At the same time, in the Barents Sea and Arctic waters, the maximum content did not exceed 0.20 mg·m^{-3}. The distribution of nutrients corresponded to that for the winter period when the vertical gradients of these parameters were not formed yet. The values of water saturation with oxygen exceeding 100% (to varying degrees throughout the studied area) characterized the activation of the photosynthesis process in the phytoplankton community. Analysis of long-term data showed that the subsequent active spring phytoplankton bloom in years with negative ice cover anomalies occurred already in the second or third decade of April in the Barents Sea water masses of various types – in Arctic, Atlantic, and coastal waters (maximum chlorophyll *a* concentration reached the value of 5.69 mg·m^{-3} in Arctic waters). In May, this process covered various types of water masses throughout the Barents Sea (maximum chlorophyll *a* content was of 5.08–5.77 mg·m^{-3}). In abnormally cold years, the low position of the ice edge in March–April limited the possible area of phytoplankton development, and the active phase of its bloom (according to satellite data) occurred much later, in May. Atlantification of the Barents Sea contributes to the formation of several bloom spots and the distribution of spring bloom over a larger area, which might affect the annual production indicators of the entire pelagic zone.

Keywords: chlorophyll *a*, spring bloom, water masses, Atlantification, Barents Sea

Climate change affects and is expected to significantly affect Arctic marine ecosystems with consequences at different levels: pelagic, benthic, and sympagic. The observed sharp warming in the Arctic Basin that began in the 1980s under the effect of global climate anomalies [Barber et al., 2008; Comiso, Hall, 2014] resulted in alterations in climatic and hydrological parameters of the Barents Sea. Recently, there has been a rise in volume and temperature of Atlantic waters entering the Barents Sea, as well as associated unprecedented reduction in sea ice and an increase in the ice-free period [Alekseev, 2015; Boitsov et al., 2012; Zhichkin, 2015].

The term "Atlantification" was first used to characterize the periodic change in the vertical structure of waters in the central Barents Sea [Reigstad et al., 2002]. Further, this concept was expanded to the entire Barents Sea, and the term was defined as an increase in the influx of Atlantic waters leading to reduction in sea ice in the sea. To date, this term is applied to the entire Nansen Basin. Intensification of Atlantification in the Arctic Ocean consists of expanding the zone of effect of Atlantic waters on its hydrological and ice regime [Aksenov, Ivanov, 2018]. The Barents Sea, being a sort of heat exchanger for the Arctic Ocean, releases most of ocean heat entering from the North Atlantic. The resulting heat exchange between air and sea is critical both for regulating climate and determining deep circulation in the Arctic Ocean and beyond. According to climate model projections, in a warming climate, the cooling role of the Barents Sea is likely to expand to the Kara Sea and then to the Arctic Basin. Accordingly, Arctic Atlantification will intensify and shift poleward in future [Shu et al., 2021].

There is still limited knowledge about climate effect on timing of the spring phytoplankton bloom onset, its duration, and levels of quantitative development of primary producers in Arctic waters. Reduction of the area of the Arctic Ocean ice is expected to result in increased primary phytoplankton production [Kahru et al., 2011; Wassmann, 2011]. It will be facilitated by a rise in ice-free water area, a longer vegetation period, and additional carbon export to the pelagic zone from the atmosphere [Lewis et al., 2020]. All these factors can affect phenology of phytoplankton blooms in the Barents Sea [Dong et al., 2020; Oziel et al., 2017]. Seasonal variations of sea ice boundaries related to a decrease in the ice cover have already led to a shift in spring and summer phytoplankton blooms in the Barents Sea in northern and eastern directions [Oziel et al., 2017].

In the Arctic and subarctic zones of the World Ocean, most of the annual primary production is formed during spring phytoplankton blooms; all further development of the ecosystem of Arctic seas during the year is determined by the level of the spring bloom. A bloom of phytoplankton is understood as an annually recurring increase in its total biomass. In the northern Barents Sea, the onset of this process is traditionally related to the ice edge zone, and in the southeastern Barents Sea, to shallow areas and streams of the main Atlantic currents [Biological Atlas, 2022; Kuznetsov, Shoshina, 2003; Plankton morei Zapadnoi Arktiki, 1997]. The bloom onset is determined by the coincidence of several physical factors: ice melting, amount of incoming light, stratification of the water column, wind mixing, nutrient supply, *etc.* [Fujiwara et al., 2014; Park et al., 2015; Wang et al., 2018]. According to different authors, the bloom begins in March-April [Biological Atlas, 2022; Qu et al., 2006] or April-May [Kuznetsov, Shoshina, 2003; Plankton morei Zapadnoi Arktiki, 1997]. The main, prevailing species are representatives of Arctic diatoms of neritic origin [Makarevich et al., 2012]. The Barents Sea spring phytoplankton bloom reaches its maximum values in May throughout the entire ice-free water area, including the area of drifting ice, and subsides in summer. Summer phytoplankton outbreaks recorded in some

cases in the ice edge zone are of a secondary, facultative nature [Biological Atlas, 2022; Kuznetsov, Shoshina, 2003; Wassmann et al., 2006]. As a rule, *in situ* studies cover only small areas of the sea (meridional or latitudinal transects), and this does not allow to conclude on the rest of the water area. A more complete picture is provided in works based on satellite observations. However, for high latitudes, obtaining satellite data is difficult due to high cloudiness and is associated with data distortion resulting from averaging.

In March–April 2021, expeditionary research was carried out in the Barents Sea ice-free water area. The aim of the work was to identify spots of early spring phytoplankton blooms. To do this, we determined chlorophyll *a* concentration: in general, its variability can reflect variability of phytoplankton biomass and serve as an indicator of total abundance and productivity of the phytoplankton community.

MATERIAL AND METHODS

The work was carried out during the cruise of the RV "Dalnie Zelentsy" from 10 March to 12 April, 2021, and covered a vast ice-free water area of the Barents Sea. In total, 9 transects were performed in the latitudinal and meridional directions, which included 52 hydrological stations and 34 complex stations (Fig. 1). The stations and transects were numbered in accordance with the RV records.

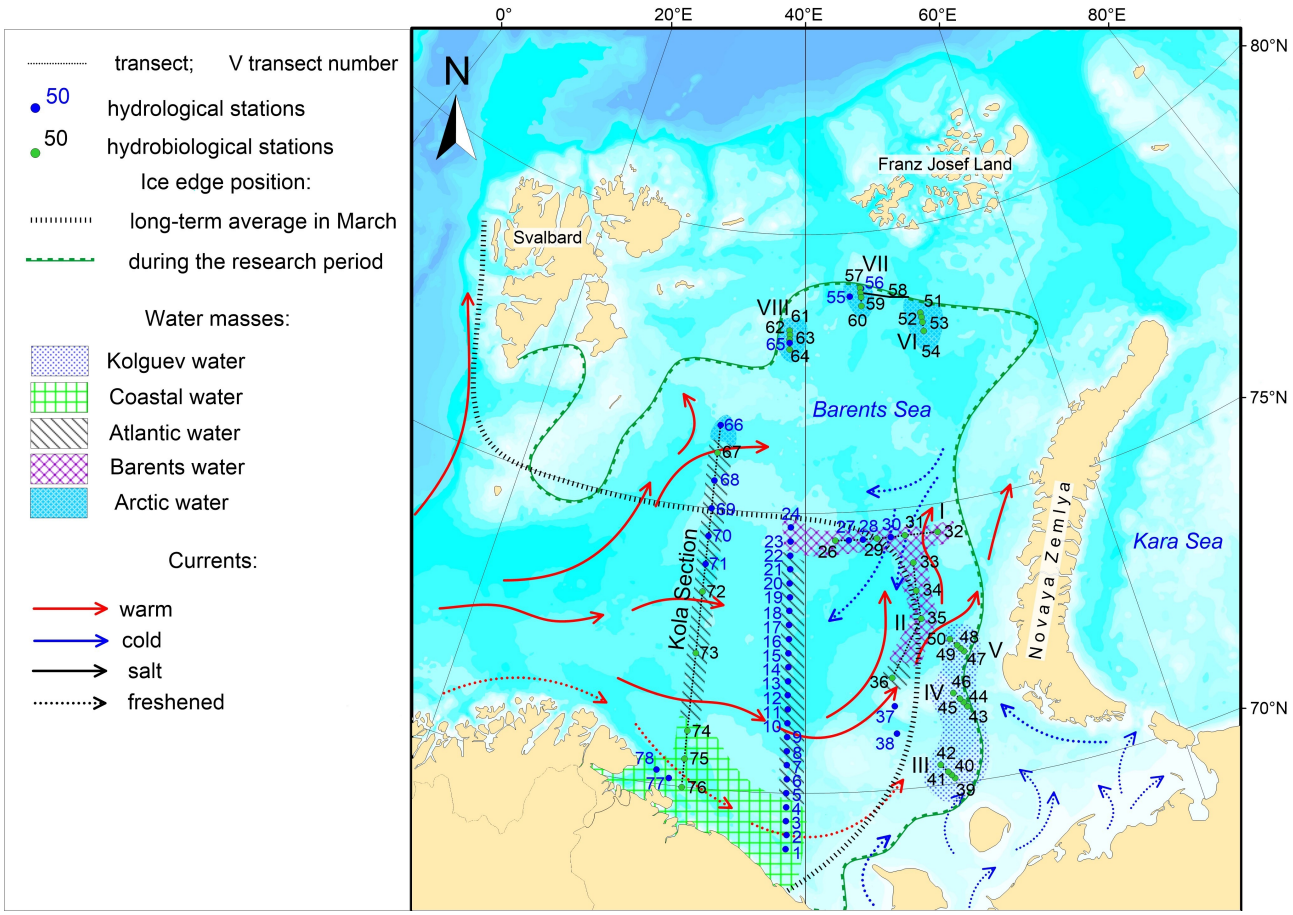

Fig. 1. Location of stations and ice conditions, the Barents Sea, March–April 2021. The ice edge location according to [EOSDIS Worldview, 2022; Johannessen et al., 2007]

To describe the hydrological structure of water masses in the studied area, material from the RV report was used [Reisovyi otchet, 2021]. At 52 stations, complex hydrological works were carried out. Water temperature and salinity were determined using SBE 19plus V2 SeaCAT Profiler (Sea-Bird Scientific, the USA). Based on the data obtained, temperature and salinity isolines along the transects were built. To isolate water masses, TS analysis was carried out [Mamaev, 1987].

For further determination of chlorophyll *a* (hereinafter Chl-*a*) concentrations ($mg \cdot m^{-3}$), seawater was sampled at horizons of 0, 25, and 50 m. Niskin bottles of 5 and 10 L were used (Hydro-Bios, Germany). A total of 114 samples were taken and processed. We followed the guideline [Aminot, Ray, 2000] based on the classic UNESCO technique for determining Chl-*a* content [Determination of Photosynthetic Pigments, 1966]. Deviations from the guideline were not allowed. Water samples of 5 L for each horizon were filtered immediately in a vacuum unit in a laboratory onboard the RV. "Vladipor" membrane filters with a diameter of 47 mm and a pore size of 0.6 μm were used. After filtration, the filters, folded in half with the sediment inward, were stored in the freezer in a desiccator with silica gel at a temperature of −20 °C. Further processing of the samples was carried out in a stationary hydrochemical laboratory. The precipitate was extracted with 90% acetone. After homogenization, the samples were centrifuged at 8,000 rpm. Chl-*a* concentration in the extract was determined on a Nicolet Evolution 500 spectrophotometer (Spectronic Unicam, the UK).

To analyze the spatial distribution of Chl-*a* concentrations for the entire sea area, satellite remote sensing data and decrypted NASA images [Ocean Color NASA, 2022] were used. Daily and averaged (monthly) data were investigated. Level-3 CHL from SeaWiFS satellites (material for 1998) and MODIS-Aqua (material for 2021) were used. Data from the NASA website were imported into the ArcMAP GIS application, and raster images of Chl-*a* spatial distribution for a certain period were formed.

For hydrochemical studies, seawater was sampled at horizons of 0, 10, 25, 50, and 100 m and in the bottom layer. Dissolved oxygen (O_2) concentrations ($mg \cdot L^{-1}$) were determined using a MARK-303 portable oxygen meter (VZOR, Russia). The acid-base balance (pH) was measured in unfiltered water samples with an I-500 ionometer (Akvilon, Russia) and adjusted to *in situ* value. Inorganic dissolved phosphorus ($P\text{-}PO_4$) was determined by the Murphy–Riley method; dissolved silicon ($Si\text{-}SiO_3$), by the Korolev method; and nitrites ($N\text{-}NO_2$) and nitrate nitrogen ($N\text{-}NO_3$), by the Bendschneider–Robinson method [Chemical Methods, 1983; Methods of Seawater Analysis, 1999; Rukovodstvo po khimicheskomy analizu, 2003]. The parameters were measured on a PE-5300VI spectrophotometer (Ecroskhim, Russia).

When analyzing the data, we used the values of content of Atlantic waters (fa, %), river waters (fr, %), and waters transformed due to ice formation/melting (fi, %). These values were obtained by calculation applying the dependencies given in the work of A. Namyatov [2021a].

The dependencies were obtained by analyzing 2,200 results of parallel determinations of salinity and the isotopic parameter $\delta^{18}O$ in 1978–2014 in the Barents Sea by various authors, at different seasons of the year, and at different horizons. The justification for the possibility of using these dependencies beyond the existing series of observations of salinity – $\delta^{18}O$ was considered by A. Namyatov [2021b].

RESULTS

Water masses on the performed transects. The Barents Sea water mass. Transects I and II were performed on 21–26 March in the Central Basin area of the Barents Sea. There, the water surface does not cool as much in winter as in the southeastern sea due to the effect of warm Atlantic currents. At the stations of transect I, the water column was well mixed from the surface to the bottom and occupied by the Barents Sea water, with the temperature of 0…–0.5 °C and salinity of 34.72–34.83 PSU (Fig. 2).

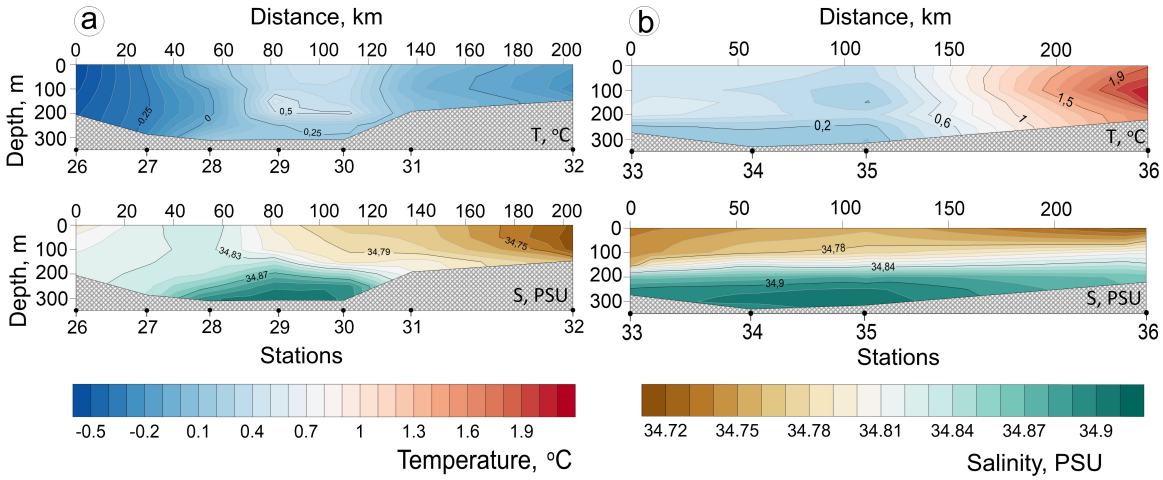

Fig. 2. Temperature (T, °C) and salinity (S, PSU) at the transects: a, transect I; b, transect II

In the deepest area of the transect (sta. 28–30) at depths of more than 150 m, there was a slight increase in temperature (up to +0.5 °C) and salinity (up to 34.91 PSU) caused by the effect of Atlantic currents. At sta. 33–35 of transect II, the mixed water layer extended to a depth of 100–150 m. Its temperature and salinity characteristics corresponded to those of the Barents Sea water. Under the mixed layer, the temperature decreased slightly, and the salinity increased. At sta. 36 at a depth of about 100 m, a warm (+2.2 °C) stream of transformed Atlantic waters of the Novaya Zemlya Current was recorded; those retained their identity only in the temperature field (not in the salinity field).

At sta. 32 of transect I, closest to the ice edge, the maximum value of dissolved oxygen saturation in water was registered, 102%. In the more western area of the transect, the value did not exceed 100%.

The Kolguyev water mass. The survey with high spatial resolution (distance between stations was 5 to 10 nautical miles) was carried out near the ice edge in the northern and southeastern Barents Sea. Transects III, IV, and V were located in the southeastern sea. The White Sea Current supplies this area with the White Sea waters, with a salinity of about 33 PSU. The highest salinity in this area is noted in November–February. A decrease in salinity related to the influx of desalinated water from the White Sea begins already in March and affects not only the surface layer, but also the intermediate and even bottom ones [Ozhigin et al., 2016]. In winter months, the Barents Sea ice-free water area is intensively cooled. Under the effect of convective and wind mixing in this period, a 100–150-m thick layer is formed, relatively uniform in terms of temperature and salinity. In shallow areas of the sea, mixing can reach the bottom. The structure of the water column becomes more complex in spring since ice begins to melt. The work was carried out there on 27–29 March, when the spring ice melting had not yet begun.

At transects III and IV, temperature and salinity rose monotonically with depth. Water surface temperature was of −1.8…−1 °C; at the bottom, temperature was close to 0 °C; and at some stations, it reached above-zero values (Fig. 3).

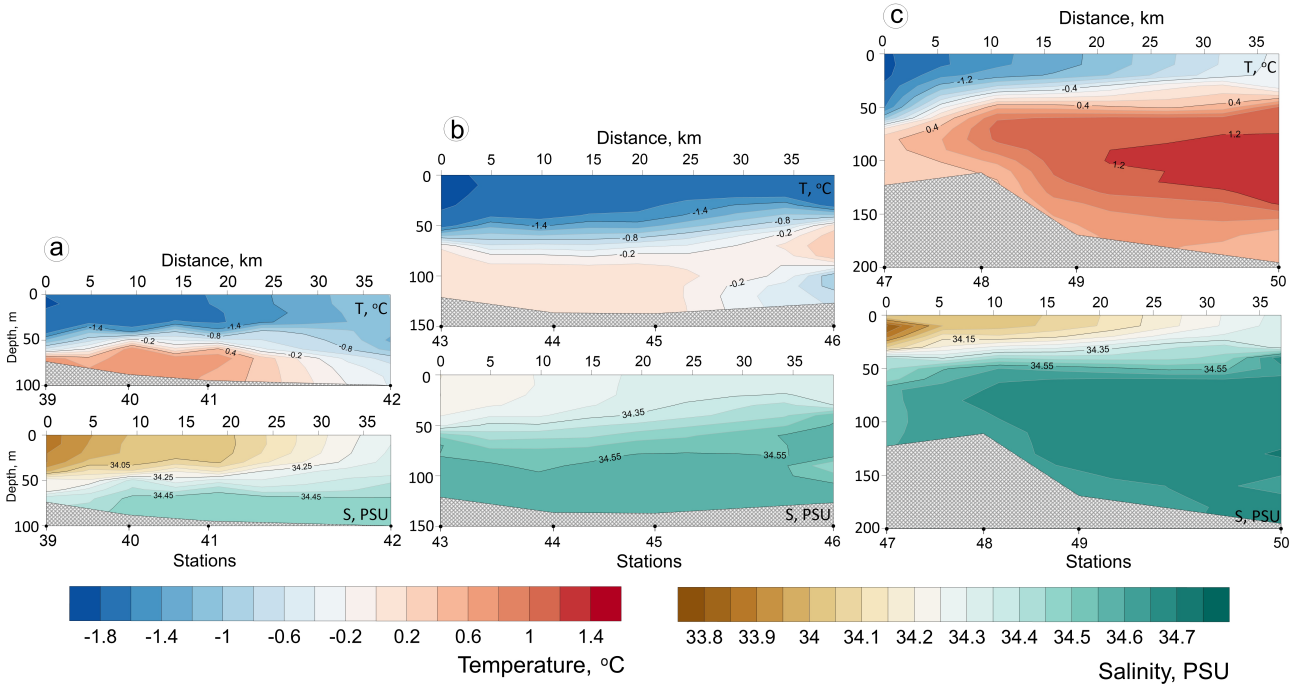

Fig. 3. Temperature (T, °C) and salinity (S, PSU) at the transects: a, transect III; b, transect IV; c, transect V

The minimum salinity value at the surface was 33.9 PSU. The maximum value at the bottom was 34.6 PSU. At transect V (sta. 49 and 50) at a depth of 100 m, a stream of warm water (+1.4 °C) with a salinity of 34.7 PSU was recorded. These stations are confined to the North Novaya Zemlya Trench, which is one of the routes for distribution of transformed Atlantic waters of the Novaya Zemlya Current. In general, the stations of transects III, IV, and V can be attributed to the Kolguyev structure of water masses. In the area of these transects, the characteristics and structure of the water column are determined primarily by the influx of desalinated waters from the White Sea, a large volume of river influx into the southeastern Barents Sea, and an intensive water mixing down to the bottom in autumn and winter.

The eastern stations of these transects were carried out in close proximity to the ice edge. At these stations, the dissolved oxygen saturation in water was lower than 100%. However, when moving away from the edge to the northwest, an excess of the threshold value of 100% was recorded, and this indicates the location of the first spring spots of the photosynthesis activation. At more southern transect III, this area is confined to the surface layer of sta. 42 (101%). At more northern transects IV and V, the area with the highest values was located in the 40–60-m layer. The maximums were 101 and 104%, respectively. The distribution of other nutrients across the transects was patchy.

The Arctic water mass. Transects VI, VII, and VIII were performed on 31 March – 3 April in the northern Barents Sea near the ice edge. In the study period, there was no layer of melted water. At transects VI and VII, the entire water column consisted of waters of Arctic origin. Temperature and salinity increased with depth, reaching –0.8 °C and 34.82 PSU at the bottom, respectively (Fig. 4).

At transect VIII, Arctic waters also prevailed, but at sta. 61 and 64, the effect of Atlantic waters was registered near the bottom. The temperature reached above-zero values (+0.5 °C). In this area, there is a complex system of currents capable of bringing both Atlantic waters from the western border of the Barents Sea and highly transformed Atlantic waters that have passed through the Arctic Basin.

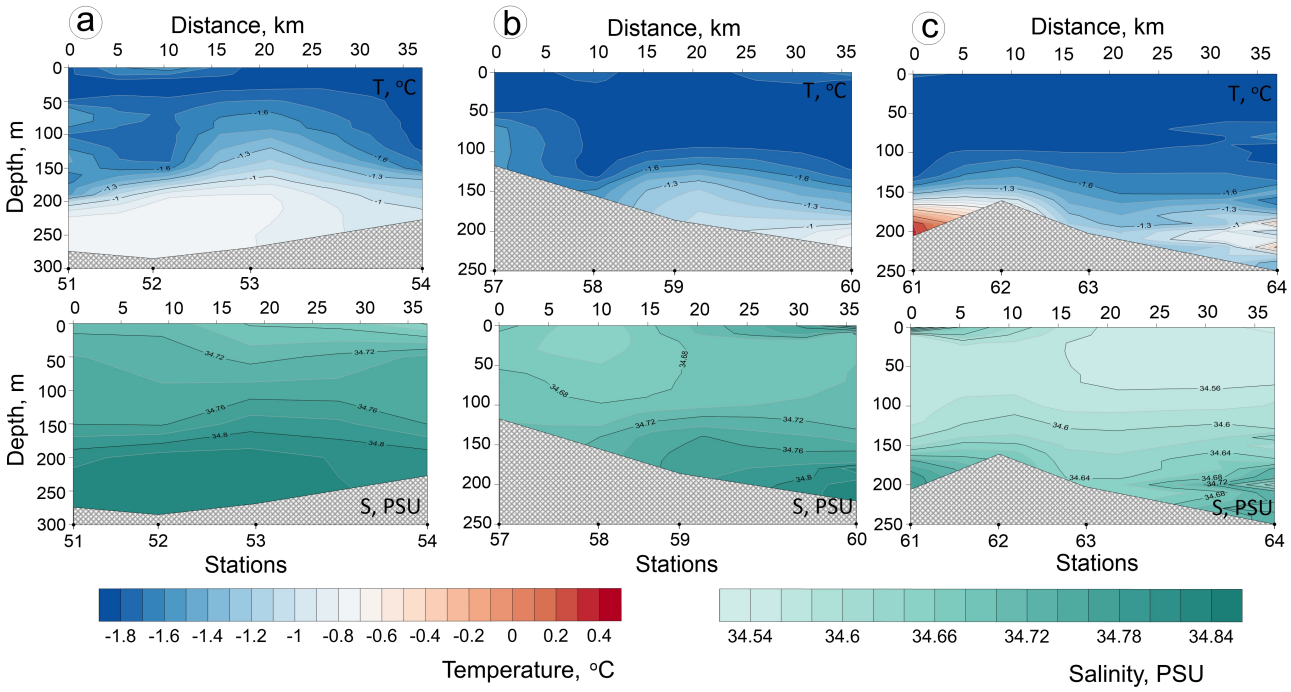

Fig. 4. Temperature (T, °C) and salinity (S, PSU) at the transects: a, transect VI; b, transect VII; c, transect VIII

Excessive oxygen saturation in water was observed in the surface layer almost throughout the entire transect VIII, which is the westernmost in this group of transects. In the surface layer of its southern area, the oxygen saturation value reached 105% (sta. 64), and an excess of the threshold value of 100% in the surface layer was observed almost throughout the entire transect. In the surface layer of other, more eastern transects in this water mass, oxygen saturation was less than 100%: the values accounted for 98–99%.

Atlantic and coastal water masses. The work at the standard oceanographic transect "Kola Meridian" was carried out on 8–12 April. The transect was located on the route of distribution of warm waters of the North Cape Current and desalinated waters of the Murmansk Coastal Current. In the southern area of the transect (sta. 74–76), there was a decrease in salinity (down to 34.44–34.65 PSU) which resulted from the freshwater runoff of the rivers of Northern Norway and the Kola Peninsula, carried by the Norwegian and Murmansk currents (Fig. 5). The distribution boundary of desalinated coastal waters was determined on the sea surface between sta. 74 and 73. In the central area of the transect (sta. 67–73), Atlantic waters of high salinity (34.95 PSU) were recorded. At sta. 66, the main water column was occupied by Arctic waters, with sub-zero temperature (−1.2 °C) and low salinity (34.44 PSU). At the bottom at sta. 66, a layer of warmer (+0.8 °C) and more saline (34.84 PSU) transformed Atlantic water was registered.

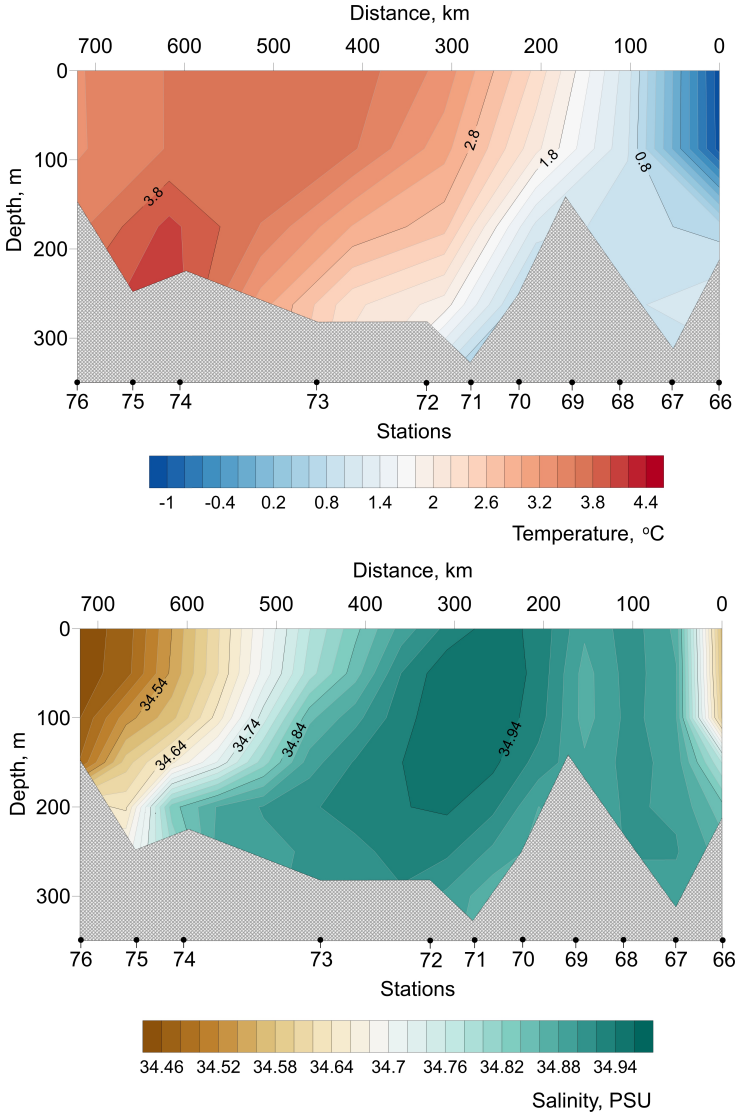

Fig. 5. Temperature (T, °C) and salinity (S, PSU) at transect "Kola Meridian"

At this transect, unlike the other ones, in the surface layer from the southern stations to northern ones, the dissolved oxygen saturation in water exceeded 100%. In the surface layer of Atlantic waters, it varied from 100 to 102%; in cold Arctic waters in the northern area of the transect, the value sharply increased to 108%.

Hydrochemical parameters of water masses. All water masses of the Barents Sea are formed by three basic waters – Atlantic ones, river ones, and waters transformed due to ice formation/melting [Namyatov, 2021a]. An alteration in the ratio of these waters throughout the year because of their advection from other water areas and vertical mixing can significantly affect the nature of the annual cycle of variability for the nutrients studied. Table 1 provides the mean values and standard deviations of concentrations of considered nutrients, temperature and salinity values, and the values of the content of Atlantic waters (fa, %), river waters (fr, %), and meltwater (fi, %) in the water masses described by us in March–April 2021.

Table 1. Mean values and standard deviations of temperature (T, °C) and salinity (S, PSU), concentrations of nutrients, and the values of the content of Atlantic waters (fa, %), river waters (fr, %), and meltwater (fi, %) in the 0–10-m layer, March–April 2021

Water mass	The Kolguyev water mass		The Barents Sea water mass		The Arctic water mass		The Atlantic water mass	The coastal water mass
	a	b	a	b	a	b	b	b
Sta. no.	39, 43, 47	40–42, 44, 46, 48–50	32	26, 29, 31	51, 57, 61, 66	52–54, 58–60, 62–64	67–73	74–76
T, °C	−1.82 ± 0.02	−1.40 ± 0.46	–0.19	−0.07 ± 0.42	−1.64 ± 0.31	−1.82 ± 0.06	2.16 ± 1.30	3.54 ± 0.05
S, PSU	34.00 ± 0.18	34.18 ± 0.14	34.72	34.8 ± 0.01	34.67 ± 0.09	34.65 ± 0.08	34.91 ± 0.04	34.49 ± 0.05
fa, %	97.0	97.5	99.1	99.2	98.9	98.8	99.6	98.4
fa, min–max, %	96.4–97.5	97.0–97.9		99.2–99.3	98.6–99.4	98.4–99.5	99.3–99.7	98.2–98.6
fr, %	2.55	2.09	0.69	0.53	0.84	0.90	0.24	1.29
fr, min–max, %	2.04–3.09	1.71–2.54		0.51–0.58	0.41–1.10	0.31–1.67	0.34–3.89	1.13–1.40
fi, %	0.49	0.43	0.23	0.21	0.26	0.29	0.16	0.33
fi, min–max, %	0.43–0.55	0.39–0.49		0.21–0.22	0.19–0.30	0.17–0.31	0.14–0.21	0.30–0.34
O_2, mL·L^{-1}	8.32 ± 0.12	8.42 ± 0.09	8.16	8.02 ± 0.08	8.48 ± 0.32	8.40 ± 0.19	7.84 ± 0.42	7.42 ± 0.04
O_2, min–max, %	97.7–100.6	98.3–107.5	99.3–101.9	100.4	97.3–108.1	105.1	98.2–108.9	99.7–101.5
P-PO_4, μM	0.36 ± 0.11	0.35 ± 0.09	0.59	0.50 ± 0.10	0.53 ± 0.08	0.47 ± 0.12	0.50 ± 0.10	0.44 ± 0.10
N-NO_3, μM	4.61 ± 1.20	5.33 ± 0.87	7.53	8.57 ± 0.33	7.18 ± 1.58	7.14 ± 0.67	10.7 ± 0.74	7.19 ± 0.61
Si-SiO_3, μM	2.67 ± 0.52	1.93 ± 0.75	2.40	1.88 ± 0.41	1.95 ± 0.31	1.55 ± 0.54	3.16 ± 0.87	2.14 ± 0.33

Note: a, stations closest to the ice edge; b, stations located in open water.

A common feature of distribution of nutrients (P-PO_4, N-NO_3, and Si-SiO_3) at all the performed transects was their correspondence to the winter type, when vertical gradients of these parameters were not formed yet. The bottom layers were characterized by the lowest values of dissolved oxygen saturation in water (up to 94%) and increased concentrations of mineral forms of phosphorus, nitrogen, and silicon.

Chlorophyll *a* concentrations at the performed transects. At transects I and II (the Barents Sea waters), Chl-*a* content in the surface layer was (0.11 ± 0.05) and (0.13 ± 0.02) mg·m^{-3}, respectively; at a depth of 25 m, (0.15 ± 0.04) and (0.16 ± 0.01) mg·m^{-3}, respectively; and at a depth of 50 m, the absolute values were comparable to those for the surface layer (Fig. 6a, b). The only station of transect II located in Atlantic waters (sta. 36), did not differ in terms of Chl-*a* concentration from other stations carried out in the Barents Sea waters.

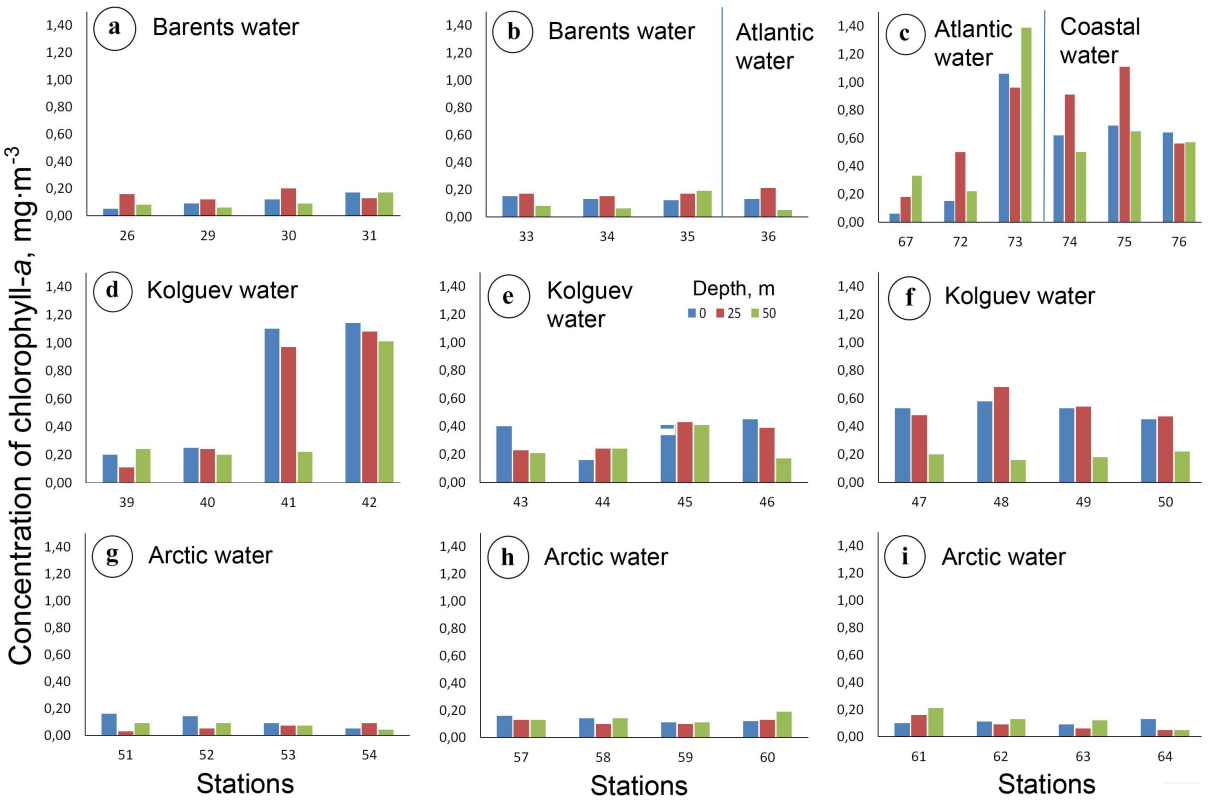

Fig. 6. Chlorophyll *a* concentrations (mg·m^{-3}) at the transects: a, transect I; b, transect II; c, transect "Kola Meridian"; d, transect III; e, transect IV; f, transect V; g, transect VI; h, transect VII; i, transect VIII

Transects III, IV, and V (Fig. 6d, e, f) performed in the southeastern Barents Sea were affected by the Kolguyev water mass. At the stations of transect III close to the ice edge (sta. 39 and 40), Chl-*a* concentrations averaged (0.23 ± 0.04) mg·m^{-3} (0 m), (0.18 ± 0.09) mg·m^{-3} (25 m), and (0.22 ± 0.03) mg·m^{-3} (50 m) (Fig. 6d). At sta. 41 and 42, Chl-*a* content rose significantly, up to 1.14 mg·m^{-3} (0 m). There, the mean values were the highest for the entire Kolguyev water mass: (0.96 ± 0.28) mg·m^{-3} (0 m), (0.87 ± 0.27) mg·m^{-3} (25 m), and (0.60 ± 0.40) mg·m^{-3} (50 m) (Fig. 6d). Sta. 41 and 42 were characterized by a slight increase in surface water temperature compared to that at sta. 39 and 40. Apparently, sta. 41 and 42 were affected by the Kola Peninsula coastal waters carried by the Murmansk Current (see Fig. 1). Thus, there might be an advection of phytoplankton from the Kola Peninsula coastal waters to the area of sta. 41 and 42. This could contribute to an earlier onset of the spring phytoplankton bloom there than at other stations in the southeastern Barents Sea. At transect IV (Fig. 6e), a decrease in Chl-*a* concentrations was recorded, while content in the 0–50-m layer varied accounting for (0.36 ± 0.13) mg·m^{-3} (0 m), (0.32 ± 0.10) mg·m^{-3} (25 m), and (0.26 ± 0.11) mg·m^{-3} (50 m). At transect V (Fig. 6f), higher Chl-*a* concentrations were observed in the surface layer, (0.52 ± 0.05) mg·m^{-3}, and at 25-m depth, (0.54 ± 0.10) mg·m^{-3}, while at a depth of 50 m, the value decreased to (0.19 ± 0.03) mg·m^{-3}.

Edge transects VI, VII, and VIII were performed in the northern water area, in Arctic waters. Low Chl-*a* concentrations, not exceeding (0.13 ± 0.02) mg·m^{-3}, were distributed relatively evenly both in the water column and between stations of all three transects (Fig. 6g, h, i).

Stations of the longest transect, “Kola Meridian” (Fig. 6c), were carried out in various water masses. Specifically, sta. 74–76 were located in coastal waters. The mean Chl-*a* concentrations were quite high throughout the 0–50-m layer: (0.65 ± 0.04) mg·m^{-3} (0 m), (0.86 ± 0.28) mg·m^{-3} (25 m), and (0.57 ± 0.08) mg·m^{-3} (50 m). The maximum Chl-*a* content was recorded at a horizon of 25 m for sta. 74 and 75: the values were of 0.91 and 1.11 mg·m^{-3}, respectively. Sta. 67, 72, and 73 were carried out in Atlantic waters. Interestingly, at sta. 73, Chl-*a* concentrations were high, with a maximum of 1.39 mg·m^{-3} (50 m). The proximity of this station to the area of coastal waters is noteworthy. There, the thermohaline characteristics of the water column were more consistent with those for Atlantic waters than with coastal ones. However, the salinity front on the sea surface passed between sta. 74 and 73, and the temperature front, between sta. 73 and 72. Thus, sta. 73 turned out to be located in the area of intense interaction between two types of water masses. High Chl-*a* content was not recorded in Atlantic waters. This suggests that its higher concentrations at sta. 73 result from the development of phytoplankton from coastal waters. At sta. 67 and 72, which were located in Atlantic waters beyond the frontal zone, the mean Chl-*a* content was low, no more than (0.34 ± 0.23) mg·m^{-3} (25 m).

According to our study results, in late March and early April 2021, the spatial distribution of Chl-*a* concentrations, as well as their absolute and mean values, differed significantly in the Barents Sea waters of various origin (Fig. 7). Like in previous studies [Makarevich et al., 2021, 2022], there was no linear relationship between variations in Chl-*a* content and temperature or salinity characteristics of water. Apparently, the dynamics of Chl-*a* concentration is related not to the thermohaline characteristics of water masses, but to their origin and migration routes. Chl-*a* content averaged for the 0–50-m layer was distributed fairly evenly within each of the identified water masses, with the exception of those at sta. 41, 42, and 73 (Fig. 7). Sta. 41 and 42 (Kolguyev waters) and sta. 73 (Atlantic waters) are most likely to have been affected by Murmansk coastal waters.

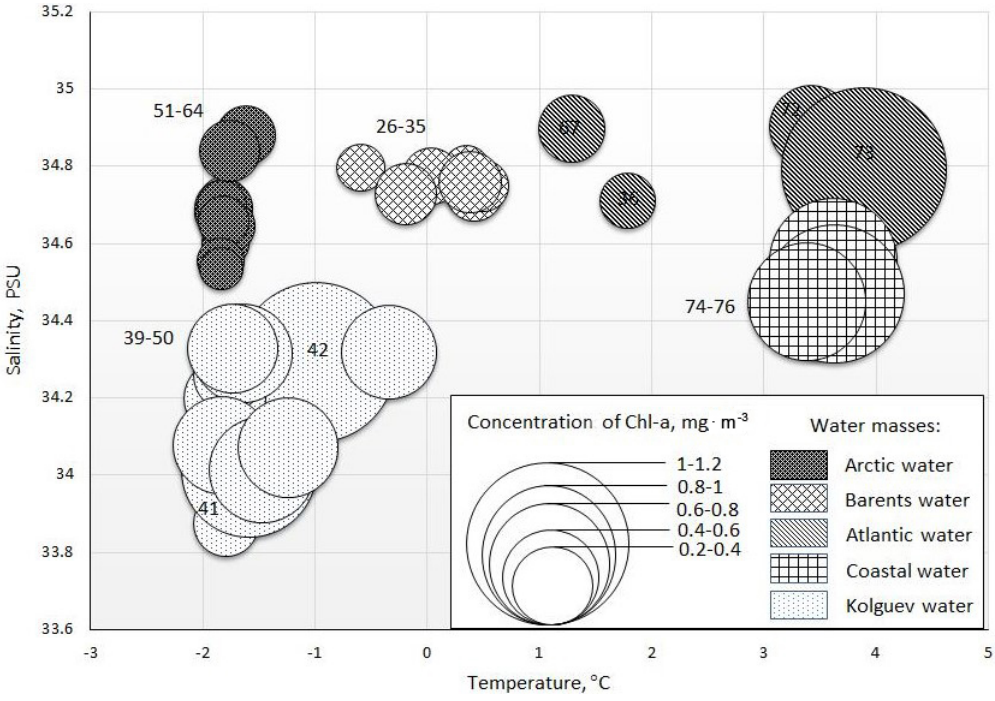

Fig. 7. Concentrations of chlorophyll *a* (Chl-*a*, mg·m^{-3}) averaged for a seawater horizon of 0–50 m on a TS diagram

DISCUSSION

Spring phytoplankton vegetation in non-freezing areas of the Barents Sea begins in late March and early April and is primarily confined to shallow water areas of the southeastern sea and waters near the ice edge [Biological Atlas, 2022]. The spring maximum of phytoplankton development is formed mainly due to early spring arctic-boreal neritic diatoms [Makarevich et al., 2012].

Phytoplankton blooms in the Barents Sea are very sensitive to seasonal and interannual changes in sea ice area and to distribution of water masses and ocean fronts [Oziel et al., 2017]. The main environmental factors affecting the Barents Sea spring phytoplankton bloom are the rapidly increasing daily total irradiance, occurrence of maximum concentrations of nutrients in the pelagic zone, vertical mixing, and position of the polar front and boundaries of the ice cover [Kogeler, Rey, 1999; Signorini, McClain, 2009]. Meltwater is an additional mechanism that triggers spring bloom in areas of melting sea ice along the Barents Sea ice edge [Dong et al., 2020; Oziel et al., 2017]. In shallow areas of the sea, an important regulating factor in the onset of the spring phytoplankton bloom is the removal of spores and phytoplankton cells from bottom sediments, while the processes of vertical mixing of the water column can contribute to the microalgae bloom in the photic layer of the pelagic zone [Eilertsen et al., 1993]. Spring bloom is an annually recurring short-term increase in phytoplankton biomass and abundance. In the open area of the Barents Sea, one spring maximum of phytoplankton development is registered. At the onset of the spring bloom, Chl-*a* concentrations in the Barents Sea first are characterized by values of about 0.5 mg·m^{-3}, and then those sharply increase. Its content can reach 6–14 mg·m^{-3} [Makarevich et al., 2022; Reigstad et al., 2002]. The maximum bloom does not last long; moreover, it is followed by a rapid decline in productivity of pelagic microalgae communities. An abundant (rapid) microalgae bloom leads to a rapid decrease in nutrient reserves in the upper layers of the pelagic zone, and the presence of sharp stratification prevents the replenishment of this reserve from underlying layers [Kuznetsov, Shoshina, 2003].

According to long-term observations, the month of the most extended ice cover for the Barents Sea is March. Usually in March, the entire eastern sea is covered with ice. In the western sea, ice extends south down to N75°. Until mid-April, the ice cover continues to increase; then, the ice edge gradually shifts to the north and east. In May, the entire central Barents Sea is ice-free; in late June and early July, the Pechora Sea and the coast of the Novaya Zemlya archipelago are ice-free [Johannessen et al., 2007]. In different years, the seasonal position of the ice edge can differ significantly from the long-term mean one. In abnormally cold years, the last of which was 1998, during the period of its maximum development, ice covered a significantly larger area of the Barents Sea and stayed longer. In such years, the southeastern sea was completely or partially covered with ice until mid-July. According to remote satellite monitoring data, low Chl-*a* content in March–April of the abnormally cold year of 1998 excluded the spring bloom stage in the phytoplankton succession cycle. Only in May, maximum Chl-*a* concentrations and active development of phytoplankton were recorded throughout the entire ice-free water area of the Barents Sea (Fig. 8). In abnormally warm years, already in late May, the Novaya Zemlya coast and the Pechora Sea can be completely ice-free. In both warm and cold years, the southwestern Barents Sea is ice-free throughout the year. In 2021, negative ice cover anomalies in the sea were registered. In May 2021, the Pechora Sea began to become ice-free; by mid-May, the Novaya Zemlya coastal waters were already completely ice-free. Data from remote satellite monitoring of Chl-*a* content for 2021 indicate as follows: in contrast to the abnormally cold year, active development of phytoplankton

was observed already in April in the southeastern Barents Sea and in certain areas of the rest of the water area. In May, the process of phytoplankton development spread in the central and northern directions and covered almost the entire sea area (Fig. 8).

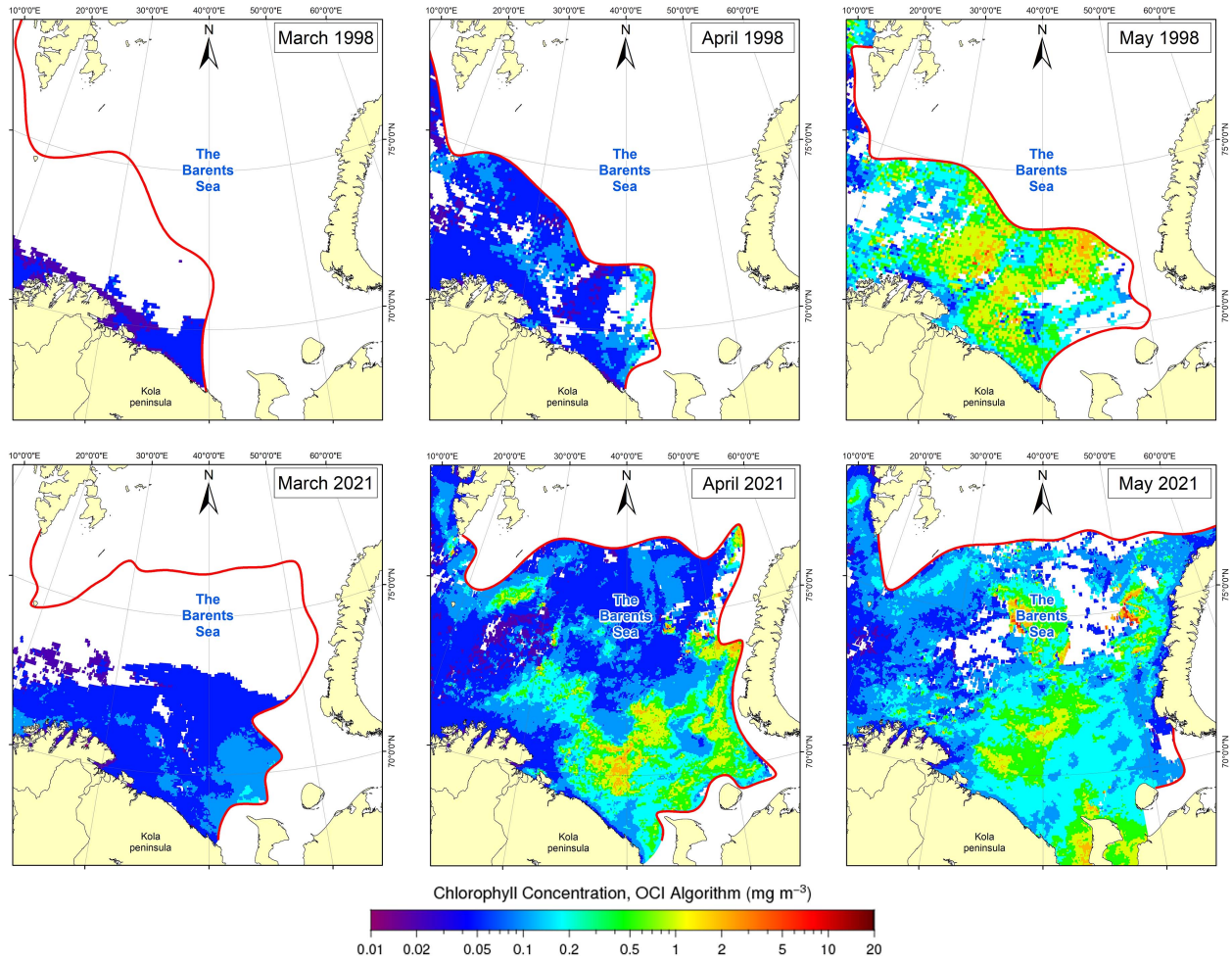

Fig. 8. Monthly averaged chlorophyll *a* concentrations (mg·m^{-3}) according to satellite data [Ocean Color NASA, 2022]. The red line is the average position of the ice edge for the month according to [EOSDIS Worldview, 2022; Johannessen et al., 2007]

Long-term *in situ* observations of the distribution of Chl-*a* concentrations in water masses of different types in the Barents Sea allowed to systematize this material for warm years. Fig. 9 shows averaged data on Chl-*a* content in various water masses (the 0–50-m layer) of the Barents Sea in spring: March 2021; April 2016, 2018, 2019 [Makarevich et al., 2022], and 2021; May 2016 and 2018 [Makarevich et al., 2021, 2022]; and July 2017 [Vodopianova et al., 2019]. The years of 2016, 2017, 2018, and 2019 were characterized by negative ice cover anomalies, and these years are comparable to 2021.

According to our data, in years with negative ice cover anomalies, the onset of the spring phytoplankton bloom can be observed already in the third decade of March and the first decade of April. The vast ice-free water area contributes to the development of this process in several isolated areas – in the southwestern and southeastern sea. Spots of increased Chl-*a* concentrations were recorded in coastal, Atlantic, and Kolguyev waters.

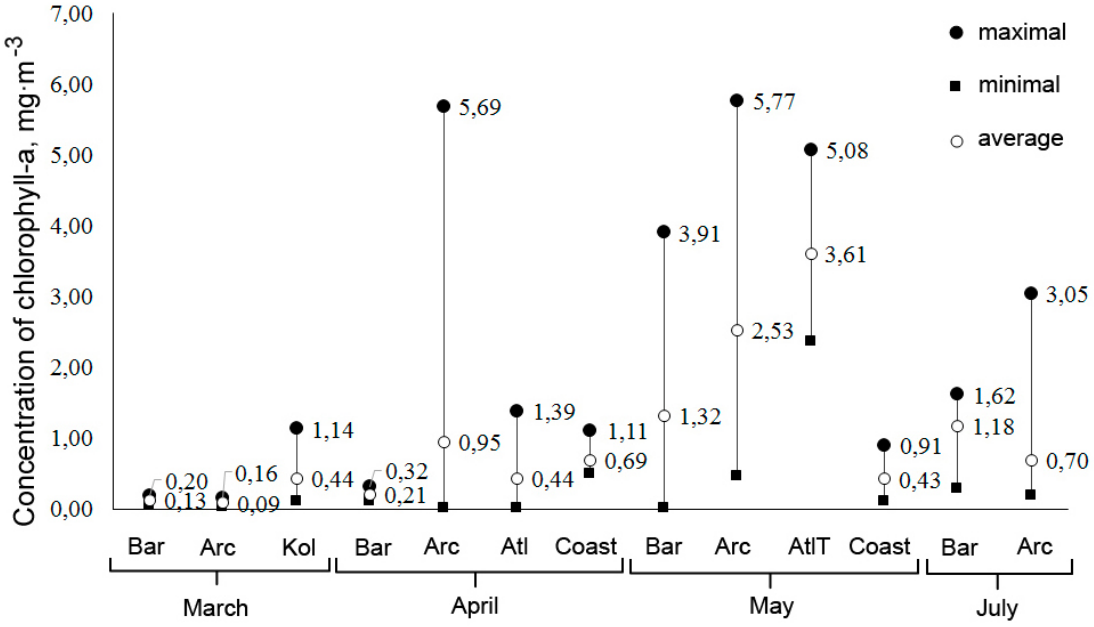

Fig. 9. Chlorophyll *a* concentrations (mg·m^{-3}) averaged for 0–50-m layer and water masses in the Barents Sea: March 2021; April 2016, 2018, 2019 [Makarevich et al., 2022], and 2021; May 2016 and 2018 [Makarevich et al., 2021, 2022]; July 2017 [Vodopianova et al., 2019] (Bar, Barents Sea waters; Kol, Kolguyev waters; Atl, Atlantic waters; AtlTw, transformed Atlantic waters; Arc, Arctic waters; CW, coastal waters)

Based on literature material, the Barents Sea coastal waters are characterized by occurrence of several outbreaks of phytoplankton development (3 to 4) during the vegetation period; however, the mean Chl-*a* content during the active development in the coastal area in the southwestern Barents Sea is low, about 1 mg·m^{-3} [Kuznetsov, Shoshina, 2003]. According to our data, in March, the mean Chl-*a* concentration in Kolguyev waters which are coastal in origin was higher than in other water masses (the mean of 0.44 mg·m^{-3}). In April, Chl-*a* content in coastal waters in the southwestern area averaged 0.64 mg·m^{-3}; in May, the value decreased to 0.43 mg·m^{-3} (Fig. 9).

In Arctic and Barents Sea waters in March, Chl-*a* concentration was very low. In the Barents Sea waters, the value averaged 0.13 mg·m^{-3}. Equally low Chl-*a* content in the Barents Sea waters was recorded in April (the mean of 0.21 mg·m^{-3}); only in May, it reached significant values (the mean of 1.32 mg·m^{-3}) (Fig. 9). In March, Arctic waters were also characterized by extremely low concentrations (the mean of 0.11 mg·m^{-3}). Already in April, a sharp increase in content was observed (the mean of 1.32 mg·m^{-3}); in May, Chl-*a* concentrations continued to rise there (the mean of 2.53 mg·m^{-3}). The maximum values in Arctic waters in April and May were 5.69 and 5.77 mg·m^{-3}, respectively. By July, we noted a decrease in content of this pigment in Arctic and Barents Sea waters, but the values still remained significant, with mean of 0.70 mg·m^{-3} (Arctic waters) and 1.18 mg·m^{-3} (the Barents Sea waters).

In April, in Atlantic waters, Chl-*a* content averaged 0.44 mg·m^{-3} (maximum of 1.39 mg·m^{-3}). In May, in transformed Atlantic waters, the pigment concentration was already noticeably higher (maximum of 5 mg·m^{-3}). This month, a generally high background of content was established in water masses of all types (Fig. 9).

Our data show as follows: in March–April 2021, vertical gradients of changes in the mineral forms of phosphorus, nitrogen, and silicon, characteristic of the period of active photosynthesis, were not formed yet. Variations in nutrient content are not always directly related to changes in phytoplankton biomass or Chl-*a* concentrations. The specific nutrient content depends on the relationship between basic waters, physical factors (seawater temperature and salinity), the position of the ice edge, and the intensity of the occurring photosynthesis process (see Table 1). In the Arctic region, during the warm season, values of dissolved oxygen saturation in water exceeding 100% are traditionally related to phytoplankton development [Khimiya okeana, 1979]. The variability of this parameter in the studied water area and the values above 100% of the level of dissolved oxygen saturation in water indicated the activation of the photosynthesis process in the phytoplankton community.

Conclusion. The spatial heterogeneity of chlorophyll *a* distribution that we observed in the spring of 2021 was due to the disunity of phytoplankton bloom spots in time and space. The location and extent of areas of increased (or decreased) chlorophyll *a* concentrations were consistent with the alternation of water masses. Its local maximums were recorded in the coastal zone of central Murman and in Kolguyev shallow waters. In the waters of the northern Barents Sea, adjacent to the ice edge, chlorophyll *a* values were significantly lower than those for the southern sea. The waters of the central sea were characterized by intermediate (average) chlorophyll *a* content.

The distribution of mineral forms of phosphorus, nitrogen, and silicon in various water masses of the Barents Sea in March–April 2021 was more consistent with the winter type, when vertical gradients of their changes were not formed yet. The values of dissolved oxygen saturation in water exceeding 100% were recorded in different sites of the water area and indirectly indicated the activation of the photosynthesis process in the phytoplankton community.

There is a dependence of the localization of spots of early spring phytoplankton development on the area of ice cover. In cold years (periods with positive ice cover anomalies), active spring phytoplankton bloom occurred late, in May. In years with negative ice cover anomalies, an outbreak of spring bloom was registered in April-May in the Barents Sea coastal waters, but the onset of this process could be observed already in the third decade of March. Against the backdrop of negative ice cover anomalies, we identified several epicenters of the onset of spring development: in coastal waters along the Murmansk coast; in the southeastern Barents Sea in Kolguyev waters, which are coastal in origin; and partly in Atlantic waters – in the areas affected by the coastal water mass. At the same time, the total productivity and absolute values of chlorophyll *a* concentrations in coastal waters were lower than during subsequent outbreaks of phytoplankton development in waters of another origin.

Monitoring of spring levels of chlorophyll *a* content in the Barents Sea allows to reveal the effect of increasing Atlantification of the sea on the spring successional cycle of phytoplankton. Precisely in spring, most of the annual phytoplankton biomass is formed, and the vector of further development during the year is determined. The increase in ice-free sea area observed since 1998 makes it possible to implement several scenarios for phytoplankton development in the Barents Sea and to cover most of the areas favorable for formation of spots of early spring phytoplankton bloom. In turn, the level of phytoplankton production established in spring can affect the productivity of all other links of the Barents Sea pelagic ecosystem.

The work was carried out within the framework of MMBI state research assignment "Structural and dynamic transformations of pelagic ecosystems of Arctic marine basins under conditions of technogenic and natural environmental changes."

Acknowledgment. The authors are grateful to the staff of the Murmansk Marine Biological Institute of the Russian Academy of Sciences for data collecting and sampling under expeditionary conditions. The authors express their deep gratitude to the reviewers for their valuable comments and suggestions.

REFERENCES

1. Aksenov P. V., Ivanov V. V. "Atlantification" as a possible cause for reducing of the sea-ice cover in the Nansen Basin in winter. *Problemy Arktiki i Antarktiki*, 2018, vol. 64, no. 1, pp. 42–54. (in Russ.). https://doi.org/10.30758/0555-2648-2018-64-1-42-54
2. Alekseev G. V. Development and amplification of global warming in the Arctic. *Fundamental'naya i prikladnaya klimatologiya*, 2015, vol. 1, pp. 11–26. (in Russ.)
3. Kuznetsov L. L., Shoshina E. V. *Phytocenoses of the Barents Sea (Physiological and Structural Characteristics).* Apatity : Izd-vo KNTs RAN, 2003, 308 p. (in Russ.)
4. Mamaev O. I. *Termokhalinnyi analiz vod Mirovogo okeana.* Leningrad : Gidrometeoizdat, 1987, 296 p. (in Russ.)
5. Ozhigin V. K., Ivshin V. A., Trofimov A. G., Karsakov A. L., Antsiferov M. Yu. *The Barents Sea Water: Structure, Circulation, Variability.* Murmansk : PINRO, 2016, 260 p. (in Russ.)
6. *Plankton morei Zapadnoi Arktiki* / G. G. Matishov (Ed.). Apatity : Murmanskii morskoi biologicheskii institut, 1997, 352 p. (in Russ.)
7. *Reisovyi otchet kompleksnoi ekspeditsii na NIS "Dal'nie Zelentsy" v Barentsevo more (10.03–14.04.2021)* / P. R. Makarevich (Ed.). Murmansk : MMBI, 2021, 99 p. (in Russ.)
8. *Rukovodstvo po khimicheskomy analizu morskikh i presnykh vod pri ekologicheskom monitoringe rybokhozyaistvennykh vodoemov i perspektivnykh dlya promysla raionov Mirovogo okeana.* Moscow : VNIRO, 2003, 202 p. (in Russ.)
9. *Khimiya okeana* : [in 2 vols]. Vol. 1: *Khimiya vod okeana*. Moscow : Nauka, 1979, 518 p. (Okeanologiya). (in Russ.)
10. Aminot A., Ray F. *Standard Procedure for the Determination of Chlorophyll a by Spectroscopic Methods.* Copenhagen, Denmark : International Council for the Exploration of the Sea, 2000, 17 p. (ICES Techniques in Marine Environmental Sciences).
11. Barber D. G., Lukovich J. V., Keogak J., Baryluk S., Fortier L., Henry G. H. R. The changing climate of the Arctic. *Arctic*, 2008, vol. 61, no. 5, suppl. 1, pp. 7–26. https://doi.org/10.14430/arctic98
12. *Biological Atlas of the Arctic Seas 2000: Plankton of the Barents and Kara Seas* / Murmansk Marine Biological Institute, Russia ; Ocean Climate Laboratory, NODC/NOAA, USA. URL: https://www.nodc.noaa.gov/OC5/BARPLANK/start.html [accessed: 20.03.2022].
13. Boitsov V. D., Karsakov A. L., Trofimov A. G. Atlantic water temperature and climate in the Barents Sea, 2000–2009. *ICES Journal of Marine Science*, 2012, vol. 69, iss. 5, pp. 833–840. https://doi.org/10.1093/icesjms/fss075
14. *Chemical Methods for Use in Marine Environment Monitoring.* Paris : UNESCO, 1983, 53 p. (Intergovernmental Oceanographic Commission Manuals and Guides ; 12). https://doi.org/10.25607/OBP-1419
15. Comiso J. C., Hall D. K. Climate trends in the Arctic as observed from space. *Climate Change*, 2014, vol. 5, iss. 3, pp. 389–409. https://doi.org/10.1002/wcc.277
16. *Determination of Photosynthetic Pigments in Sea-Water.* Paris : UNESCO, 1966, 69 p. (Monographs on Oceanographic Methodology ; vol. 1).

17. Dong K., Kvile Ø. K., Stenseth N. C., Stige L. C. Associations among temperature, sea ice and phytoplankton bloom dynamics in the Barents Sea. *Marine Ecology Progress Series*, 2020, vol. 635, pp. 25–36. https://doi.org/10.3354/meps13218
18. Eilertsen H.-C., Hansen G. A., Svendsen H., Hegseth E. N. Onset of the spring phytoplankton bloom in the Barents Sea: Influence of changing light regime and other environmental factors. *Proceedings of SPIE : Underwater Light Measurements*, 1993, vol. 2048, pp. 20–32. https://doi.org/10.1117/12.165507
19. *EOSDIS Worldview* : [site]. URL: https://worldview.earthdata.nasa.gov [accessed: 25.03.2022].
20. Fujiwara A., Hirawake T., Suzuki K., Imai I., Saitoh S.-I. Timing of sea ice retreat can alter phytoplankton community structure in the western Arctic Ocean. *Biogeosciences*, 2014, vol. 11, iss. 7, pp. 1705–1716. https://doi.org/10.5194/bg-11-1705-2014
21. Johannessen O. M., Alexandrov V. Yu., Frolov I. Ye., Sandven S., Pettersson L. H., Bobylev L. P., Kloster K., Smirnov V. G., Mironov Ye. U., Babich N. G. *Remote Sensing of Sea Ice in the Northern Sea Route. Studies and Applications.* Chichester, UK : Praxis Publishing, 2007, 472 p. https://doi.org/10.1007/978-3-540-48840-8
22. Kahru M., Brotas V., Manzano-Sarabia M., Mitchell B. G. Are phytoplankton blooms occurring earlier in the Arctic? *Global Change Biology*, 2011, vol. 17, iss. 4, pp. 1733–1739. https://doi.org/10.1111/j.1365-2486.2010.02312.x
23. Kogeler J., Rey F. Ocean colour and the spatial and seasonal distribution of phytoplankton in the Barents Sea. *International Journal of Remote Sensing*, 1999, vol. 20, iss. 7, pp. 1303–1318. https://doi.org/10.1080/014311699212740
24. Lewis K. M., van Dijken G. L., Arrigo K. R. Changes in phytoplankton concentration now drive increased Arctic Ocean primary production. *Science*, 2020, vol. 369, no. 6500, pp. 198–202. https://doi.org/10.1126/science.aay8380
25. Makarevich P., Druzhkova E., Larionov V. Primary producers of the Barents Sea. In: *Diversity of Ecosystems* / A. Mahamane (Ed.). London, UK : InTech Open, 2012, pp. 367–393. https://doi.org/10.5772/37512
26. Makarevich P. R., Vodopianova V. V., Bulavina A. S. Dynamics of the spatial chlorophyll-*a* distribution at the Polar Front in the marginal ice zone of the Barents Sea during Spring. *Water*, 2022, vol. 14, iss. 1, art. no. 101 (23 p.). https://doi.org/10.3390/w14010101
27. Makarevich P. R., Vodopianova V. V., Bulavina A. S., Vashchenko P. S., Ishkulova T. G. Features of the distribution of chlorophyll-*a* concentration along the western coast of the Novaya Zemlya archipelago in spring. *Water*, 2021, vol. 13, iss. 24, art. no. 3648 (14 p.). https://doi.org/10.3390/w13243648
28. *Methods of Seawater Analysis* / K. Grasshoff, K. Kremling, M. Ehrhardt (Eds). Weinheim ; New York ; Chichester ; Brisbane ; Toronto : Wiley-VCH, 1999, 600 p. https://doi.org/10.1002/9783527613984
29. Namyatov A. A. $\delta^{18}O$ as a tracer of the main regularities of water mass mixing and transformation in the Barents, Kara, and Laptev seas. *Journal of Hydrology*, 2021a, vol. 593, art. no. 125813 (18 p.). https://doi.org/10.1016/j.jhydrol.2020.125813
30. Namyatov A. A. The relationship between geophysical processes and changes in the composition of the seawater of the Barents Sea in the course of their climatic variability. *ESS Open Archive*, 2021b, 38 p. https://doi.org/10.1002/essoar.10507159.1
31. *Ocean Color NASA* : [site]. URL: https://oceancolor.gsfc.nasa.gov/l3/ [accessed: 25.03.2022].
32. Oziel L., Neukermans G., Ardyna M., Lancelot C., Tison J.-L., Wassmann P., Sirven J., Ruiz-Pino D., Gascard J.-C. Role for Atlantic inflows and sea ice loss on shifting phytoplankton blooms in the Barents Sea. *Journal of Geophysical Research Oceans*, 2017, vol. 122, iss. 6, pp. 5121–5139. https://doi.org/10.1002/2016JC012582

33. Park J., Kug J., Bader J., Rolph R., Kwon M. Amplified Arctic warming by phytoplankton under greenhouse warming. *The Proceedings of the National Academy of Sciences of the United States of America*, 2015, vol. 112, no. 19, pp. 5921–5926. https://doi.org/10.1073/pnas.1416884112
34. Qu B., Gabric A. J., Matrai P. A. The satellite-derived distribution of chlorophyll-*a* and its relation to ice cover, radiation and sea surface temperature in the Barents Sea. *Polar Biology*, 2006, vol. 29, iss. 3, pp. 196–210. https://doi.org/10.1007/s00300-005-0040-2
35. Reigstad M., Wassmann P., Riser C., Øygarden S., Rey F. Variations in hydrography, nutrients and chlorophyll *a* in the marginal ice-zone and the central Barents Sea. *Journal of Marine Systems*, 2002, vol. 38, iss. 1–2, pp. 9–29. https://doi.org/10.1016/S0924-7963(02)00167-7
36. Shu Q., Wang Q., Song Z., Qiao F.-L. The poleward enhanced Arctic Ocean cooling machine in a warming climate. *Nature Communications*, 2021, vol. 12, art. no. 2966 (9 p.). https://doi.org/10.1038/s41467-021-23321-7
37. Signorini S. R., McClain C. R. Environmental factors controlling the Barents Sea spring–summer phytoplankton blooms. *Geophysical Research Letters*, 2009, vol. 36, iss. 10, art. no. L10604 (5 p.). https://doi.org/10.1029/2009GL037695
38. Vodopianova V. V., Vaschenko P. S., Bulavina A. S. Monitoring of chlorophyll-*a* concentration in the ice edge zone of the Barents Sea in 2017–2018. *IOP Conference Series: Earth and Environmental Science*, 2019, vol. 263, art. no. 012005 (8 p.). https://doi.org/10.1088/1755-1315/263/1/012005
39. Wang Y., Xiang P., Kang J.-H., Ye Y.-Y., Lin G.-M., Yang Q.-L., Lin M. Microphytoplankton community structure in the western Arctic Ocean: Surface layer variability of geographic and temporal considerations in summer. *Hydrobiologia*, 2018, vol. 811, iss. 1, pp. 295–312. https://doi.org/10.1007/s10750-017-3500-0
40. Wassmann P. Arctic marine ecosystems in an era of rapid climate change. *Progress in Oceanography*, 2011, vol. 90, iss. 1–4, pp. 1–17. https://doi.org/10.1016/j.pocean.2011.02.002
41. Wassmann P., Reigstad M., Haug T., Rudels B., Carroll M. L., Hop H., Gabrielsen G. W., Falk-Petersen S., Denisenko S. G., Arashkevich E., Slagstad D., Pavlova O. Food webs and carbon flux in the Barents Sea. *Progress in Oceanography*, 2006, vol. 71, iss. 2–4, pp. 232–287. https://doi.org/10.1016/j.pocean.2006.10.003
42. Zhichkin A. P. Peculiarities of interannual and seasonal variations of the Barents Sea ice coverage anomalies. *Russian Meteorology and Hydrology*, 2015, vol. 40, iss. 5, pp. 319–326. https://doi.org/10.3103/S1068373915050052

ЛОКАЛИЗАЦИЯ ЦЕНТРОВ РАННЕВЕСЕННЕГО ЦВЕТЕНИЯ ФИТОПЛАНКТОНА В ПЕЛАГИАЛИ БАРЕНЦЕВА МОРЯ

П. Р. Макаревич, В. В. Водопьянова, А. С. Булавина, П. С. Ващенко, А. А. Намятов, И. А. Пастухов

Мурманский морской биологический институт РАН, Мурманск, Российская Федерация
E-mail: *makarevich@mmbi.info*

«Атлантификация» Баренцева моря приводит к уменьшению площади ледяного покрова и увеличению периода открытой воды. Этот процесс влияет на всю пелагическую экосистему Баренцева моря, где основная часть годовой первичной продукции фитопланктона формируется во время весеннего цветения. Концентрация хлорофилла *a* отражает изменения биомассы фитопланктона и может служить показателем его продукционных характеристик. Весной 2021 г.

на свободной ото льда акватории Баренцева моря были исследованы гидрологические характеристики водных масс и особенности распределения концентрации хлорофилла *a* и биогенных элементов. Этот год характеризовался отрицательными аномалиями ледовитости. Расположение и протяжённость зон повышенных (или пониженных) концентраций хлорофилла *a* согласовались с чередованием водных масс. Были выявлены разобщённые центры ранневесеннего цветения — в прибрежных водах на юго-востоке и юго-западе Баренцева моря. В конце марта — начале апреля максимальные концентрации хлорофилла *a* в прибрежных водах достигали значений около 1 мг·м$^{-3}$. В это же время в баренцевоморских и арктических водах максимум концентраций не превышал 0,20 мг·м$^{-3}$. Распределение биогенных элементов соответствовало таковому в зимний период, когда вертикальные градиенты этих параметров ещё не сформировались. Величи́ны насыщения вод кислородом выше уровня 100 % (в разной степени на всей исследованной акватории) характеризовали активизацию процесса фотосинтеза в фитопланктонном сообществе. Анализ многолетних данных свидетельствует, что последующее активное весеннее цветение фитопланктона в годы с отрицательными аномалиями ледовитости наступало уже во второй-третьей декаде апреля в различных типах водных масс Баренцева моря — в арктических, атлантических и прибрежных водах (максимум концентраций хлорофилла *a* достигал 5,69 мг·м$^{-3}$ в арктических водах). В мае процесс весеннего цветения охватывал уже всю акваторию Баренцева моря и все типы водных масс (максимум концентраций хлорофилла *a* — 5,08–5,77 мг·м$^{-3}$). В аномально холодные годы низкое положение ледовой кромки в марте — апреле ограничивало возможную область развития фитопланктона, а активная фаза его цветения (согласно спутниковым данным) наступала гораздо позже, в мае. «Атлантификация» Баренцева моря способствует распространению весеннего цветения фитопланктона на большей акватории, что может влиять на годовые продукционные показатели всей пелагиали.

Ключевые слова: хлорофилл *a*, весеннее цветение, водные массы, «атлантификация», Баренцево море